Rare Metal Materials and Engineering
Volume 51, Issue 2, February 2022
Available online at www.rmme.ac.cn

Science Press

Cite this article as: Guo Yanjun, Yang Xiaojing, Qin Siyuan, et al. Molecular Dynamics Study on the Influence of Amorphous Layer on Single Crystal Germanium Nano-cutting[J]. Rare Metal Materials and Engineering, 2022, 51(02): 436-441.

ARTICLE

Molecular Dynamics Study on the Influence of Amorphous Layer on Single Crystal Germanium Nano-cutting

Guo Yanjun, Yang Xiaojing, Qin Siyuan, Zhou Zhe

Faculty of Mechanical and Electrical Engineering, Kunming University of Science and Technology, Kunming 650500, China

Abstract: Composite structure with amorphous layer and crystalline substrate is important for nano-machining. In order to study the influence of amorphous layer structure on the nano-cutting mechanism and mechanical properties of single crystal germanium (Ge), molecular dynamics (MD) simulations were carried out on the nano-cutting process of amorphous-crystalline layered structure (A-C model) with different amorphous layer thicknesses. Cutting force fluctuation, stress status, subsurface damage characteristics and material removal, which are the key issues in nano-machining were analyzed. The result shows that as the thickness of amorphous germanium (A-Ge) increases, the cutting force and stress decrease, and the cutting temperature increases. The plasticity of the material is enhanced as the thickness of A-Ge increases, which is due to the softening of A-Ge when the cutting temperature rises. When the thickness of A-Ge is the same as the cutting depth, the material has lower subsurface damage and higher material removal rate, so it has excellent mechanical properties.

Key words: nano-machining; single crystal germanium; amorphous-crystalline layered structure (A-C model); subsurface damage; material removal

Single crystal Ge is a typical representative of infrared optical materials, and is widely used in infrared optical and electronic applications[1,2]. Conventionally, single crystal Ge is fabricated through grinding and polishing, but these approaches are not suitable for machining axisymmetric surfaces with complex profiles. Instead, single point diamond turning (SPDT) is more promising as a deterministic method of reproduction to generate optical surfaces with high form accuracy[3,4]. Due to its hard and brittle nature, the surface fractures and short tool life are still serious problems to be solved for nanosurface acquisition of infrared optical materials[5,6].

It has been proven that single crystal Ge can be removed in a ductile mode when the material is under high hydrostatic pressure, and then optical surface quality can be achieved[7,8]. However, to achieve the perfect surface quality, appropriate processing parameters are required. This ductile cutting process can only be carried out when the undeformed chip thickness is less than the critical ductility-brittle transition (DBT) depth[9,10]. According to Lai ' s[11] research, a certain thickness of amorphous structure will appear on the machined surface of single crystal Ge during ultra-precision turning. It is believed that the amorphous structure is formed by the transformation of the metal phase caused by the intensive hydrostatic pressure during loading[12]. Therefore, the processed crystal actually has an amorphous crystal instead of its original lattice. Due to different mechanical properties, the amorphous layer on the top of the crystals can affect the machining process significantly such as ultra-precision turning, grinding and polishing. Besides, the amorphous layer can also be used to facilitate the machining of brittle materials. For example, using the method of ion implantation to form a modified layer on the surface of some hard-brittle materials (e. g, Ge, Si), the structure of the modified layer is mainly amorphous. The surface modification of ion implantation is achieved by bombarding the surface of the workpiece with high energy ion beam and destroying its initial lattice[13]. The method of nanometric machining of ion implanted materials (NiIM) can effectively increase the brittle-plastic transition thickness of the material and improve its

Received date: February 08, 2021
Foundation item: National Natural Science Foundation of China (51765027)
Corresponding author: Yang Xiaojing, Ph. D., Professor, Faculty of Mechanical and Electrical Engineering, Kunming University of Science and Technology, Kunming 650500, P. R. China, E-mail: xjyang@vip.sina.com

ultra-precision machining performance, and its validity has been proved[14].

It is obvious that the amorphous layer has a great contribution to nano-machining, while the current study cannot fully explain the phenomena and mechanisms in material removal. Therefore, in this study, molecular dynamics (MD) simulation was used to study the effect of the amorphous layer on nanometric cutting of single crystal Ge. The effects of different thicknesses of the amorphous layer on the cutting force, stress state, subsurface damage and material deformation during nano-cutting were analyzed. The purpose of this work is also to determine the thickness of the amorphous layer suitable for nano-machining.

1 Simulation Method

A numerical simulation was conducted using the MD method. In this section, the cutting model and details of making the layered composite structure were presented. Then, cutting parameter information was reported.

1.1 Nanometric cutting model

The cutting model consists of cubic diamond single crystal Ge and rigid diamond tools, as illustrated in Fig. 1. The workpiece has a size of 22.628 nm×14.143 nm×11.314 nm and includes three kinds of atoms: Newtonian atoms, thermostat atoms and boundary atoms. Nanometric cutting was performed on the Newtonian layer. The thermostat layer imitated a heat sink with a temperature of 298 K. The boundary layer imposed boundary constraints in the x and y directions to prevent the Ge atoms from moving during the cutting process. Dynamic relaxation was performed to allow the model to be in an equilibrium state before the cutting. Three different atomic interactions in the current simulation of cutting process are shown in Table 1[15,16].

Tersoff potential can be described as follows:

$$E=\sum_{i=j}V_{ij}=\sum_{i=j}f_{\mathrm{c}}(r_{ij})\left[f_{\mathrm{R}}(r_{ij})+b_{ij}f_{\mathrm{A}}(r_{ij})\right] \quad (1)$$

where E is the total energy, V_{ij} represents the potential energy between atoms i and j, r_{ij} stands for the distance between atom i and atom j, f_{R} describes a repulsive pair potential, f_{A} represents an attractive pair potential, and f_{c} is a smooth cut off function.

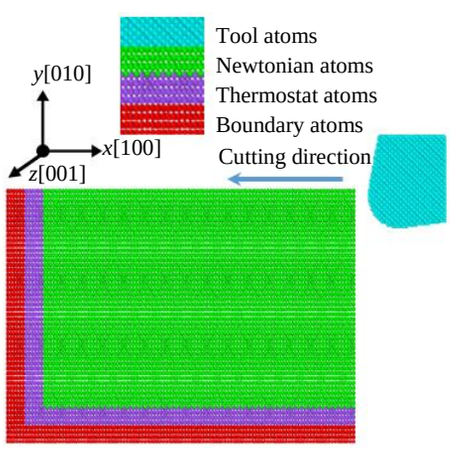

Fig.1 Schematic of the MD simulation model

Table 1 Interatomic potential

Atomic interaction	Interatomic potential
Ge-Ge	Tersoff
Ge-C	Morse
C-C	Ignore

The Morse potential can be expressed as follows:

$$V(r_{ij})=D\left\{\exp\left[-2\alpha(r_{ij}-r_0)\right]-2\exp\left[-\alpha(r_{ij}-r_0)\right]\right\} \quad (2)$$

where $V(r_{ij})$ represents the pair energy function; α and D corresponds to the elastic modulus and the cohesion energy, respectively; r_0 represent the equilibrium distance between atoms i and j. The parameter values of the Morse potential function are[17]: D=0.125 78 eV, α=25.8219 nm^{-1}, γ_0=0.223 24 nm^{-1}.

1.2 Amorphous and layered model construction

The amorphous phase was prepared by quenching[18,19]. The Ge atoms were first heated to 5000 K in 100 ps. Then, amorphous Ge atoms were obtained with a rapid cooling at 100 K. Finally, the Ge atoms were relaxed to eliminate the residual stress and balance the internal energy.

Fig. 2 shows the construction and variety of the layered model. Amorphous Ge and crystalline Ge are sliced to get amorphous and crystalline parts according to the specific thicknesses of t_{A} and t_{C}. After the joining followed by a dynamic relaxation, the model reaches equilibrium. Four A-C models with different amorphous layer thicknesses were used to study the influence of amorphous layer structure on single crystal Ge nano-cutting.

1.3 Simulation parameters

In this study, the cutting velocity is 200 m/s, which is unrealistically high in comparison with real ultra-precision scratching experiments in order to save computational cost. However, many works have confirmed that MD simulations of scratches with relatively higher scratching speed can reveal the main characteristics of the subsurface deformation mechanism[20,21]. The thickness of amorphous layers in the A-C model established was 0, 1, 2, 4 nm. More parameters used in

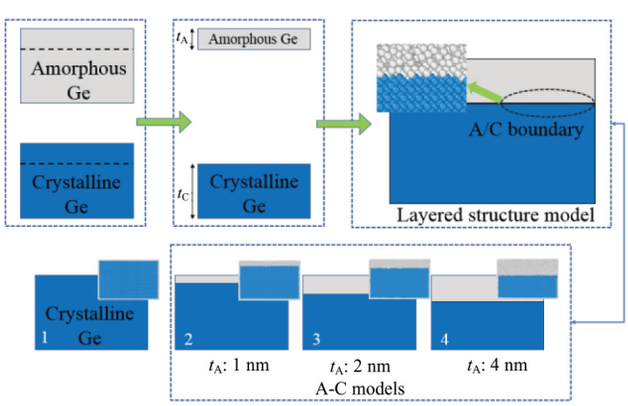

Fig.2 Construction of layered model

the present simulation are listed in Table 2. All MD simulations were performed using an open source code LAMMPS software[22]. The results of MD simulations were visualized by the OVITO software[23].

2 Results and Discussion

2.1 Characteristic of cutting forces

Fig. 3 describes the result of cutting force during the whole cutting process for different amorphous layer thicknesses. The lateral force (in the *z*-direction) is not summarized since it fluctuates around an average value of zero during the cutting process due to the balanced forces from two sides of the groove. It is found that the cutting force for different amorphous layer thicknesses increases as the tool cuts into the workpiece in phase I, as shown in Fig. 3a and 3b. As the tool continuously cuts the workpiece in phase II, the cutting force in the tangential and normal directions fluctuates around a constant value after chip formation. The fluctuations of cutting force is related to the phase change, formation and movement of dislocation in Ge. In addition, with increases of the thickness of the amorphous layer, the fluctuation amplitude of the tangential force and normal force curves in the stable cutting stage is reduced, but the fluctuation amplitude of the tangential force decreases more significantly.

To further quantify the difference of force during the nano-cutting process, both the tangential cutting force and normal cutting force are averaged over the cutting distance from 5 nm to 15 nm where cutting is in phase II for different amorphous layer thicknesses, as show in Fig. 3c. It can be seen that both the tangential cutting force and normal cutting force decrease with increases of amorphous layer thickness. This is because the amorphous structure on the surface of single crystal Ge will reduce the surface hardness and elastic modulus. Through the above analysis, it can be concluded that increasing the thickness of the amorphous layer on the surface of the workpiece can reduce the cutting force significantly, which is beneficial to the cutting process.

Fig. 3d shows the friction coefficient in phase II. It can be seen that when the amorphous layer thickness is less than the cutting depth, the friction coefficient decreases with the thickness of the amorphous layer; but as the thickness of the amorphous layer exceeds the cutting depth, the friction coefficient increases with the thickness of the amorphous layer.

Under the condition that the thickness of the amorphous

Table 2 Parameters for the MD simulation with single crystal Ge as the workpiece material and diamond as the tool material

Parameter	Value
Dimension of workpiece/nm	22.63×14.14×11.31
Tool rake angle/(°)	10
Tool back angle/(°)	7
tool nose radius/nm	2
Depth of cut/nm	2
Amorphous layer thickness/nm	0, 1, 2, 4
Cutting speed/m·s^{-1}	200
Cutting distance/nm	0~15
Initial temperature/K	298
Time step/fs	1

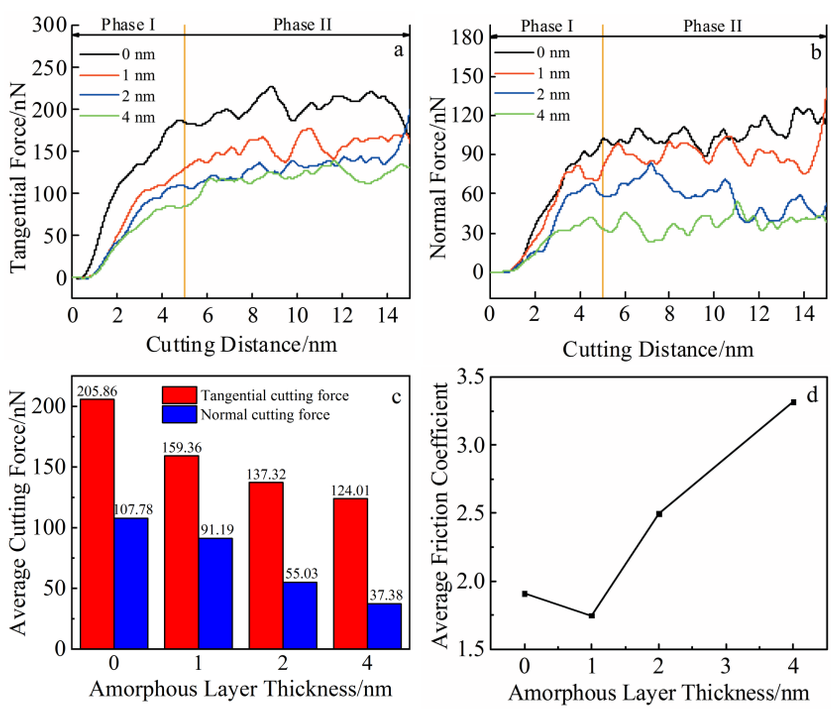

Fig.3 Machining forces of amorphous layer models with different thicknesses: (a) tangential force, (b) normal force, (c) average cutting force, and (d) average friction coefficient

layer is less than the cutting depth, increasing the thickness of the amorphous layer can reduce the tangential force; when the thickness of the amorphous layer exceeds the cutting depth, the rough amorphous surface increases the friction between the tool and the workpiece.

2.2 Characteristic of stress distribution during cutting

Shear strain can characterize the degree of deformation of the material, which can be obtained by calculating the relative amount of the current atomic configuration and the atomic configuration of the previous frame or frames by Ovito software. Fig. 4 represents the atomic strain at different amorphous layer thicknesses. As shown in Fig. 4a, the shear strain is concentrated in three distinct regions (represented by I, II and III): the rake face of the tool, the cutting area and clearance face of the tool, and there is also a narrow shear strain concentration band at the bottom of the chip. This is because the cutting edge pushes Ge atoms during the cutting process to increase the strain energy in the cutting area. When the strain energy is large enough, the atomic lattice structure fails, the Ge atoms with high strain energy expands to the region with smaller strain energy, leading to the plastic flow, so that the chip and the clearance face form a narrow shear strain band. Besides, as the thickness of the amorphous layer increases, the shear strain in the cutting zone is weakened, especially in region I, and there is also a higher shear strain at region III because of the friction between the flank and workpiece surface.

Fig. 5 shows the shear stress inside the material with different amorphous layer thicknesses. It can be seen that the shear stress is mainly concentrated at the front end of the cutting zone, and the maximum shear stress is about 4 GPa. With the increases of the amorphous layer thickness on the surface of the workpiece, the area and stress values of the shear stress concentration region decrease, which indicates that increases of the amorphous layer thickness can soften the surface of the workpiece and enhance the plasticity, and that the amorphous atoms undergo plastic flow to reach the stress value for chip generation.

2.3 Characteristic of subsurface damage under different thicknesses of amorphous layers

Fig. 6 shows the subsurface damage of the machined surface of the workpiece with different thicknesses of amorphous layers. The figure does not show the subsurface damage of the workpiece with an amorphous layer thickness of 4 nm, which is considered to be the largest damage, because the thickness of the amorphous layer is greater than the depth of cut. It can be seen that there is an amorphous periodic expansion damage zone on the subsurface, in which the expansion direction of amorphous atoms in the *x*-*y* plane is $[\bar{1}\bar{1}0]$ and $[1\bar{1}0]$, and the angle is about 90°, which is because the direction of splitting and sliding of Ge atoms is [110]. The maximum damage depth of single crystal Ge is 1.5 nm, and as the thickness of the amorphous layer increases, the maximum damage depth decreases and the tendency of amorphous atoms to expand in the *x*-*y* plane is weakened significantly. This indicates that the appropriate thickness of the amorphous layer on the workpiece surface can inhibit the downward expansion of amorphous atoms, thereby reducing the damage to the subsurface. As shown in Fig. 6c, when the thickness of the amorphous layer is close to the depth of cut, the depth of subsurface damage is the smallest, and desirable machinability at the nanoscale will be achieved.

The temperature-displacement curve during cutting process is also shown in Fig.7. The cutting heat is generated due to the friction behavior between the tool and the workpiece. During the cutting process, the cutting temperature gradually increases. In addition, it can be clearly seen that the temperature of the workpiece rises with increase in the thickness of the amorphous layer. This is because the thermal conductivity of the amorphous phase is lower than that of the crystalline phase. It is speculated that thermal softening may also be a reason for the plasticity enhancement of A-Ge.

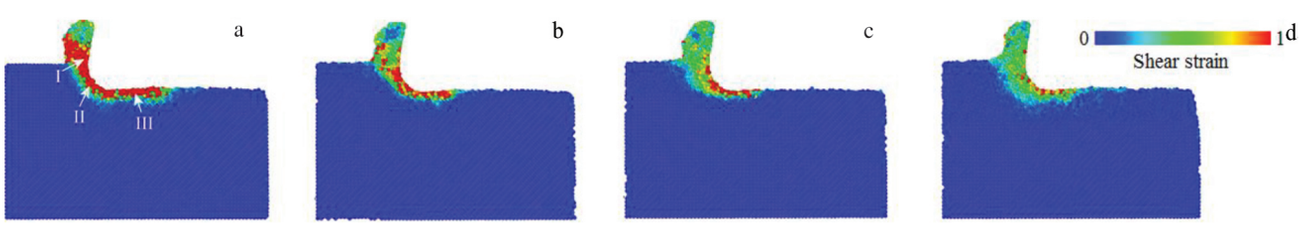

Fig.4 Atomic strains of amorphous layer models with different thicknesses : (a) 0 nm, (b) 1 nm, (c) 2 nm, and (d) 4 nm

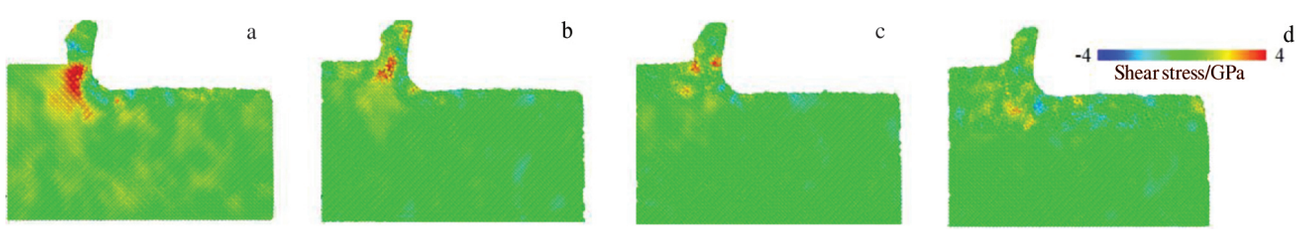

Fig.5 Stress fields of amorphous layer models with different thicknesses: (a) 0 nm, (b) 1 nm, (c) 2 nm, and (d) 4 nm

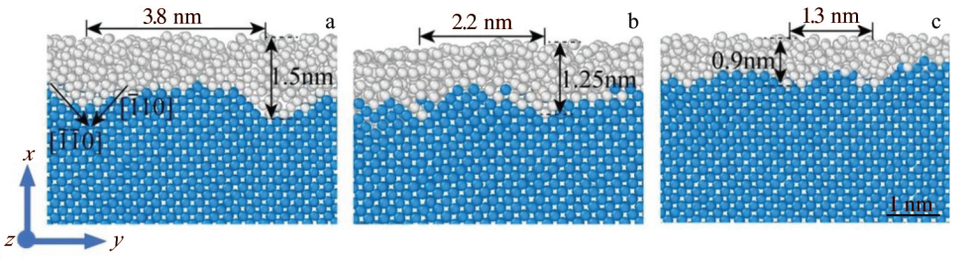

Fig.6 Subsurface damage under different thicknesses of amorphous layer: (a) 0 nm, (b) 1 nm, and (c) 2 nm

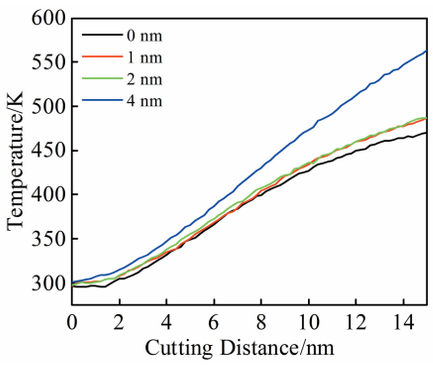

Fig.7 Temperature-displacement curves under different thicknesses of the amorphous layer

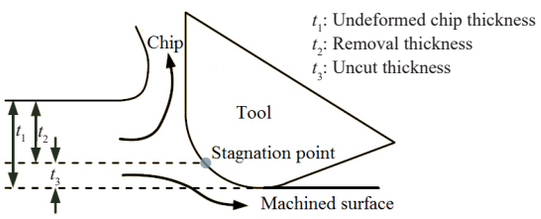

Fig.8 Uncut thickness evaluation

2.4 Uncut thickness and elastic recovery rate under different thicknesses of amorphous layers

In this work, the influence of the amorphous layer on the machining quality was analyzed by comparing the uncut thickness and elastic recovery rate during the cutting process. According to Lai's research[24], there is a stagnation point where the branching of the plastic flow occurs during the nano-cutting process. The material below this point will be pressed under the tool, and only the material above this point can flow to form chips. Fig.8 shows the evaluation method of uncut thickness. According to this method. Fig. 9 shows the uncut thickness and elastic recovery rate of the cutting models with different amorphous layer thicknesses.

It can be seen from Fig.9 that the uncut thickness of the A-C model is less than that of the C-Ge, which means a higher material removal rate. The uncut thickness decreases first and then increases with increasing the amorphous layer thickness. When the thickness of the amorphous layer is the same as the cutting depth, the uncut thickness reaches the lowest value, indicating that the material removal rate is the highest at this time.

At the same time, it is found that the elastic recovery rate also has the same trend. The elastic recovery rate of the processed area is the smallest when the thickness of the amorphous layer and the cutting depth are the same, indicating that the workpiece surface has a small amount of spring back and a small shape error under this condition. This has high significance and application value in ultra-precision processing. Therefore, the composite structure with this special thickness of the amorphous layer is preferred.

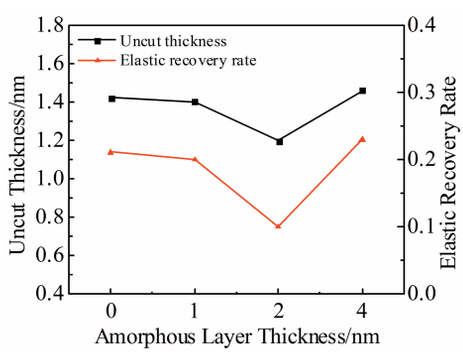

Fig.9 Uncut thickness and elastic recovery rate at different amorphous layer thicknesses

3 Conclusions

1) For the A-C model, the hardness and elastic modulus decrease with increase of the A-Ge thickness, which can reduce the stress and cutting force significantly and is beneficial to the ductile machining of brittle materials. The friction between the amorphous surface and the tool is bigger, which causes the cutting temperature to rise.

2) As the thickness of A-Ge increases, the plasticity of the material increases, which is caused by the softening of A-Ge when the cutting temperature rises.

3) The A-C model (t_A=2 nm) with specific configurations has low subsurface damage, high material removal rate and small spring back during nano-cutting, which is beneficial for processing materials at the micro-nano scale.

References

1 Fang F Z, Zhang X D, Weckenmann A *et al. CIRP Annals-Manufacturing Technology*[J], 2013, 62(2): 823
2 Hu X K, Li Y F, Fang F Z *et al. Optics Letters*[J], 2013, 38(12): 2053
3 Hatefi S, Abou-El-Hossein K. *The International Journal of Advanced Manufacturing Technology*[J], 2020, 111(9-10): 2667
4 Hatefi S, Abou-El-Hossein K. *International Journal of Advanced Manufacturing Technology*[J], 2020, 106(5-6): 2167
5 Wang J S, Fang F Z, Zhang X D. *Precision Engineering*[J], 2015, 39: 220
6 Fang F Z, Chen Y H, Zhang X D *et al. CIRP Annals-Manufacturing Technology*[J], 2011, 60(1): 527
7 Blake P N, Scattergood R O. *Journal of the American Ceramic Society*[J], 1990, 73(4): 949
8 Blackley W S, Scattergood R O. *Precision Engineering*[J], 1991, 13(2): 95
9 Yan J W, Asami T, Harada H *et al. Precision Engineering*[J], 2008, 33(4): 378
10 Yan J W, Asami T, Harada H *et al. CIRP Annals-Manufacturing Technology*[J], 2012, 61(1): 131
11 Lai M, Zhang X D, Fang F Z *et al. Precision Engineering*[J], 2017, 49: 160
12 Han J, Sun J P, Fang L. *Tribology*[J], 2016, 36(5): 562
13 Fang F Z, Chen Y H, Zhang X D *et al*. *CIRP Annals-Manufacturing Technology*[J], 2011, 60(1): 527
14 Wang J S, Fang F Z, Zhang X D. *Precision Engineering*[J], 2015, 39: 220
15 Tersoff J. *Physical Review B*[J], 1989, 39: 5566
16 Zhu P Z, Fang F Z. *Applied Physics A*[J], 2012, 108(2): 415
17 Luo L, Yang X J, Liu N *et al*. *Rare Metal Materials and Engineering*[J], 2019, 48(4): 1130
18 Kluge M D, Ray J R, Rahman A. *Physical Review B*[J], 1987, 36(8): 4234
19 Ishimaru M, Munetoh S, Motooka T. *Physical Review B*[J], 1997, 56(23): 15 133
20 Goel S, Luo X C, Reuben R L. *Computational Materials Science* [J], 2012, 51(1): 402
21 Zhang J J, Sun T, Yan Y D *et al*. *Applied Surface Science*[J], 2008, 254(15): 4774
22 Plimpton S. *Journal of Computational Physics*[J], 1995, 117(1): 1
23 Stukowski A. *Modelling and Simulation in Materials Science and Engineering*[J], 2010, 18(1): 15 012
24 Lai M, Zhang X D, Fang F Z *et al*. *Nanoscale Research Letters* [J], 2013, 8(1): 1

非晶层对单晶锗纳米切削影响的分子动力学研究

郭彦军，杨晓京，秦思远，周　哲

(昆明理工大学 机电工程学院，云南 昆明 650500)

摘　要：为探究非晶层结构对单晶锗纳米切削机制和力学特性的影响，采用分子动力学方法模拟不同非晶层厚度的非晶-晶体层状结构（A-C模型）的纳米切削过程。对纳米加工中切削力波动规律，应力状态，亚表面损伤和材料去除等关键问题进行分析。结果表明：非晶锗（A-Ge）厚度的增加使得切削力和应力减小，切削温度升高；材料的可塑性随着A-Ge厚度的增加而增强，这是由于切削温度升高时A-Ge的软化所致；当A-Ge的厚度与切削深度相同时，材料具有较低的亚表面损伤和较大的材料去除率，因此具有优异的力学性能。

关键词：纳米加工；单晶锗；非晶-晶体层状结构；亚表面损伤；材料去除

作者简介：郭彦军，男，1995年生，博士生，昆明理工大学机电工程学院，云南 昆明 650500，E-mail：xsbgyj2017@163.com